PHYSICAL REVIEW B VOLUME 60, NUMBER 4 15 JULY 1999-II

# Polarization-dependent resonant-x-ray diffraction in charge- and orbital-ordering phase of $Nd_{1/2}Sr_{1/2}MnO_3$

K. Nakamura, T. Arima, and A. Nakazawa
*Institute of Materials Science, University of Tsukuba, Tsukuba 305-8573, Japan*

Y. Wakabayashi
*Photon Factory, Institute of Materials Structure Science, High Energy Accelerator Research Organization, Tsukuba 305-0801, Japan*

Y. Murakami
*Photon Factory, Institute of Materials Structure Science, High Energy Accelerator Research Organization, Tsukuba 305-0801, Japan*
*and Core Research for Evolutional Science and Technology (CREST), Tsukuba 305-0047, Japan*

(Received 29 January 1999)

A study of resonant-x-ray scattering in a charge-ordered perovskite manganese oxide $Nd_{1/2}Sr_{1/2}MnO_3$ was performed. Dipole-resonant superlattice reflections originating from the orderings of the charge and orbital with $Q_{\rm charge}=(0,1,0)$ and $Q_{\rm orbital}=(0,1/2,0)$ in the $Pbnm$ setting were observed. Sudden change in the intensity of the superlattice scattering at the transition temperature indicated a strong first-order phase transition. Characteristic dependence on the x-ray polarization was observed not only for orbital-order superlattice scattering but also for charge-order scattering. It should be closely related to the orbital-ordering type $(d_{3x^2-r^2}/d_{3y^2-r^2})$ or $(d_{x^2-z^2}/d_{y^2-z^2})$. [S0163-1829(99)10027-4]

Colossal negative magnetoresistance (CMR) in some perovskite-type manganese oxides[1] is ascribed to the magnetic-field-induced melting of a charge ordering. The charge ordering which is widely observed in $R_{1/2}A_{1/2}MnO_3$ ($R$ is rare earth, $A$ is alkaline earth), is suggested to be accompanied by the ordering of the degrees of freedom of orbital and spin configuration of Mn $3d$ electrons.[2,3] It is very important to investigate the orbital states in order to understand the CMR and other interesting phenomena in the manganese oxide system.

$Nd_{1/2}Sr_{1/2}MnO_3$ is one of the typical charge-ordering oxides showing CMR. The structure is of an orthorhombically distorted perovskite type with the $Pbnm$ space group.[4] At room temperature it is a paramagnetic metal and shows a ferromagnetic phase transition at $T_C = 255$ K. After further cooling, a first-order metal-insulator transition is observed at charge-ordering temperature $T_{CO} \sim 150$ K.[5] A neutron-diffraction study has revealed the so-called CE-type antiferromagnetic spin ordering below $T_{CO}$ (see the arrows in Fig. 1).[6] Alternating arrangement in the $a$-$b$ plane of the spin moments at Mn sites 3 $\mu_B$ and 2.8 $\mu_B$ has also been reported, which implies a charge ordering. The observed wave vectors are (0,1,0), (1/2,0,1), and (1/2,1/2,1) for the ordering of charge, $Mn^{3+}$ spin moments of 3 $\mu_B$, and $Mn^{4+}$ spin moments of 2.8 $\mu_B$, respectively. The complicated spin structure suggests that the orbital degree of freedom also shows antiferromagnetic-ordering as shown in Fig. 1. An abrupt jump of the lattice parameters at $T_{CO}$ (Ref. 4) also indicates orbital ordering accompanied by a cooperative Jahn-Teller distortion of $Mn^{3+}O_6$ octahedra. In fact, ordering of the Jahn-Teller distortion in a relevant manganite compound $La_{1/2}Ca_{1/2}MnO_3$ has been observed using synchrotron x-ray powder diffraction,[3] which strongly indicates the $(d_{3x^2-r^2}/d_{3y^2-r^2})$-type orbital ordering.

Recently, Murakami *et al.* confirmed orbital ordering in the $K_2NiF_4$ (layered perovskite)-type manganese oxide $La_{1/2}Sr_{3/2}MnO_4$ by using the anisotropy of the tensor of susceptibility (ATS) scattering technique,[7] which is one of the resonant x-ray-diffraction techniques. The ATS technique utilizes the fact that the anomalous x-ray scattering factor of $Mn^{3+}$ near the $K$ edge behaves as a tensor rather than a scalar. The susceptibility tensor of $Mn^{3+}$ is modulated with an alternating ordering of the orbital degrees of freedom, which causes orbital superlattice scattering. However, the ATS technique has not been able to determine the type of orbital ordering, $(d_{x^2-z^2}/d_{y^2-z^2})$ or $(d_{3x^2-r^2}/d_{3y^2-r^2})$, since the orbital superlattice reflection is caused only by a difference of the tensor of susceptibility.

In this paper, we will report the observation of orbital and charge ordering in $Nd_{1/2}Sr_{1/2}MnO_3$ [as shown in Fig. 1(a)] using the resonant x-ray scattering technique. We utilized (a) an anomalous dispersion of the atomic scattering factor of Mn near the $K$-absorption edge and (b) the anisotropy of the atomic scattering factor of $Mn^{3+}$ ion with the $d_\varepsilon^3 d_\gamma^1$ configuration. Temperature dependence of the intensities of superlattice reflections shows that the orderings of charge and orbital are concomitant first-order phase transition. We will also report the characteristic dependence of the intensity of superlattice reflections on the polarization of incident x ray. Not only an orbital-ordering reflection but also a charge-ordering reflection is much stronger for the $E \| a$ configuration than for the $E \| c$ configuration. This should be strongly related to the $(d_{3x^2-r^2}/d_{3y^2-r^2})$-type orbital ordering.

A crystal of $Nd_{1/2}Sr_{1/2}MnO_3$ was melt grown using a floating-zone furnace. Twin mosaic was inevitable in the crystal. A polished $(110)_{\rm cubic}$ surface in the pseudocubic setting of a twinned sample was used for the x-ray study. The surface area was about 5 mm$\phi$. X-ray-diffraction measure-

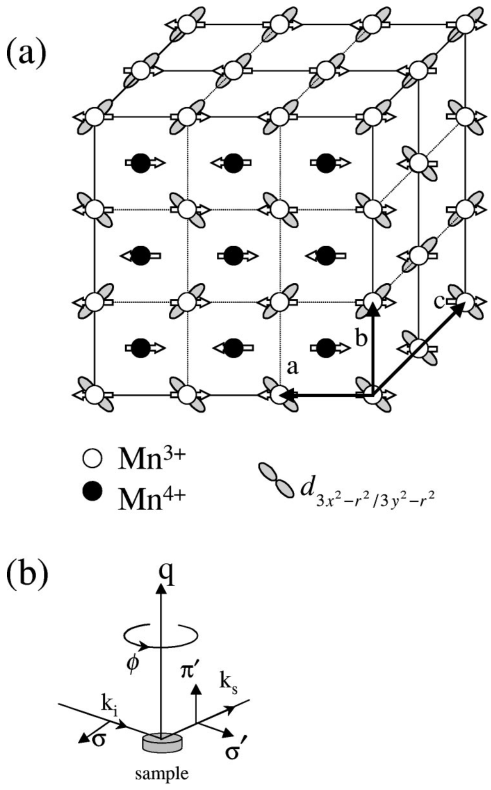

FIG. 1. (a) Schematic figure of ordering of the spin, charge, and orbital degree of freedoms in a perovskite manganese oxide $Nd_{1/2}Sr_{1/2}MnO_3$. Arrows, solid (open) circles, and wings attached with the open circles represent spins, tetra(tri)valent manganese ions, and occupied $3d_\gamma$ orbitals, respectively. The coordinate is in the $Pbnm$ setting. (b) Configuration for the present x-ray scattering experiment. The incident beam was $\sigma$ polarized. The direction of the scattering vector ($\vec{q}$) was identical with the $b$ direction of the crystal.

ments were performed on beamline 4C at the Photon Factory, KEK, Japan. The incident beam was monochromatized by Si (111) double crystals and focused by a bent cylindrical mirror. The typical energy resolution of the incident beam was 2 eV. The $\sigma$-polarized incident beam [Fig. 1(b)] was focused on the sample mounted in a closed-cycle He refrigerator on a four-axis diffractometer. Polarization analysis of the scattered beam was performed using a Cu (220) analyzer crystal, which gives a scattering angle of 95.6° for the photon energy of Mn *K* edge.

Spectra of the x-ray superlattice reflection were analyzed using the atomic scattering factor of $Mn^{3+}$ [$f_{Mn^{3+}}(\omega)$], $Mn^{4+}$ [$f_{Mn^{4+}}(\omega)$], and $O^{2-}$ ions ($f_{O^{2-}}$). For Mn ions, energy dependence of the anomalous atomic scattering factor was taken into account: x-ray-absorption spectra in $LaMnO_3$ and $SrMnO_3$ were used as the imaginary part of $f_{Mn^{3+}}(\omega)$ and $f_{Mn^{4+}}(\omega)$, respectively. The real part is calculated from the imaginary part using the Kramers-Kronig relation.

Some superlattice reflections of charge and orbital ordering were observed with the photon energy of 6.555 keV at 6 K. Hereafter all the indices are in the $Pbnm$ setting. Superlattice scattering of (0,odd,0) can be attributed to the ordering of charge because of the polarization of the scattered x ray and spectra shown below.[7] The scattered beam is $\sigma'$ polarized [see Fig. 1(b)] as in the case of normal x-ray diffraction. The (0,3/2,0) and (0,5/2,0) orbital-order reflections were also detected, while neither (3/2,0,0) nor (5/2,0,0) peaks were found, as can be expected from the model shown in Fig. 1. The (0,5/2,0) reflection were analyzed to be 68% $\pi'$ polarized, which is quite a contrast to the $\sigma'$-polarized charge-order reflections.[8]

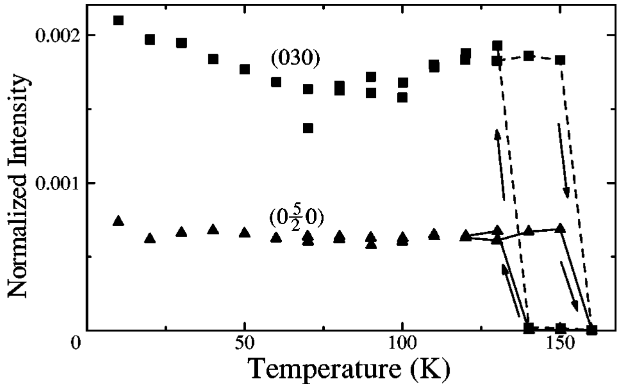

FIG. 2. Temperature dependence of the intensity of a charge and orbital superlattice scattering (0,3,0) and (0,5/2,0). The photon energy is tuned to be resonant with Mn *K* edge, as large as 6.555 keV. The polarization of the incident beam is perpendicular to the *a* axis ($\phi = 90°$). The intensities are normalized by the (0,2,0) Bragg reflection.

Figure 2 shows the intensity of the (0,3,0) and (0,5/2,0) superlattice scattering normalized by the intensity of the (0,2,0) Bragg as a function of temperature. On warming, both of the reflections show little change in intensity below 150 K and then suddenly disappear at 160 K. On a cooling run, the reflections appear again at 140 K. The temperature dependence with a hysteresis agrees with a previously-reported resistivity curve.[5] Furthermore, for the whole temperature range below $T_{CO}$, the widths of the (0,3,0) and (0,5/2,0) peaks are around 0.003 $Å^{-1}$, as narrow as the (0,2,0) Bragg. The charge and orbital ordering should coherently extend at least over 1000 Å even just below $T_{CO}$.

The solid triangles in Fig. 3 show spectra for (0,5/2,0), (0,1,0), and (0,3,0) at 6 K. Here the effect of x-ray absorption is corrected. All the spectra show a maximum around 6.555 keV, which is 3 eV above the *K*-absorption edge of $Mn^{3+}$. This strongly indicates that these reflections should be ascribed to some modulation of the Mn electronic states. One can identify this resonance with electric dipole transition (Mn $1s$–$4p$) but not with quadrupole transition ($1s$–$3d$), which should be located ~14 eV below the edge. Ishihara and Maekawa pointed out that the orbital-order reflection originated from anisotropy of the *K*-absorption energy of $Mn^{3+}$ with the $d_\varepsilon^3 d_\gamma^1$ configuration.[9] Assuming that the anisotropy is small, the scattering factor corresponding with the period of the orbital alternation should be proportional to $df_{Mn^{3+}}/d\omega$. In fact, the (0,5/2,0) spectrum qualitatively coincides with $|df_{Mn^{3+}}/d\omega|^2$ [solid line in Fig. 3(a)]. In addition to the characteristic structure near the *K* edge, a finite background is observed in the (0,1,0) and (0,3,0) spectra but not in (0,5/2,0). A regular displacement of some atoms should account for the background. The cooperative breathing and Jahn-Teller distortion of $MnO_6$ octahedra should be caused by the charge and orbital ordering, respectively. With the former distortion each oxygen between $Mn^{3+}$ and $Mn^{4+}$

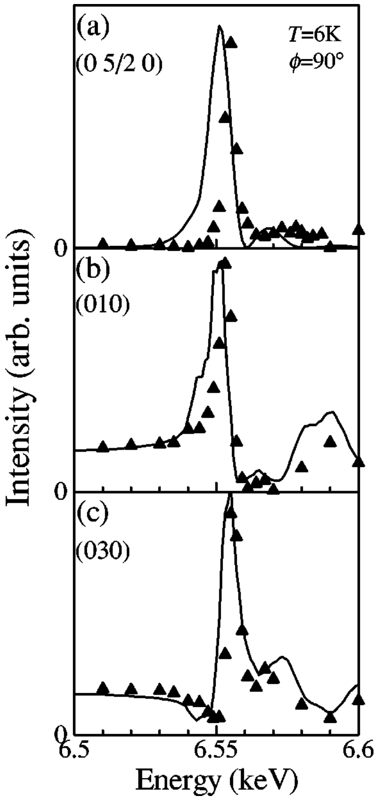

FIG. 3. Triangles denote spectra of the intensity of the (a) (0,5/2,0), (b) (0,1,0), and (c) (0,3,0) superlattice scattering, respectively, at 6 K. The polarization of the incident beam is perpendicular to the $a$ axis ($\phi=90°$). Solid lines denote the best-fitted curves calculated by (a) $|df_{\mathrm{Mn}^{3+}}/d\omega|^2$ and (b) Eq. (1).

should move towards the $\mathrm{Mn}^{4+}$ and cause the background of the (0,odd,0) superlattice scattering. It is worth noting that the Jahn-Teller distortion does not allow orbital reflections. Thus the (0,odd,0) and (0,odd/2,0) reflections can be respectively identified as originating from charge and orbital ordering. Analogous energy dependence has also been reported for charge- and orbital-order scattering in the layered manganite $\mathrm{La}_{1/2}\mathrm{Sr}_{3/2}\mathrm{MnO}_4$.[7]

The magnitude of breathing-type distortion $\varepsilon$ can be estimated from the (0,1,0) and (0,3,0) spectra. The solid lines in Figs. 3(b) and 3(c) were fitted using the energy-dependent structure factor of a charge-order superlattice reflection

$$F_{0k0}(\omega)=f_{\mathrm{Mn}^{3+}}(\omega)-f_{\mathrm{Mn}^{4+}}(\omega)-4f_{\mathrm{O}^{2-}}\sin\frac{\varepsilon k\pi}{2}, \quad (1)$$

with $\varepsilon=0.017$. This indicates that the $\mathrm{Mn}^{3+}$–O bonds in the $a$-$b$ plane should be on average 3–4% longer than the $\mathrm{Mn}^{4+}$-O bonds. The shift of ~2 eV between the fitting and experimental lines may be due to the difference of absorption energies of $\mathrm{Mn}^{3+}$ and/or $\mathrm{Mn}^{4+}$ between the sample and the reference compounds. The estimated value of the breathing-type distortion is comparable with the previous-reported powder-diffraction study in $\mathrm{La}_{1/2}\mathrm{Ca}_{1/2}\mathrm{MnO}_3$.[3]

Since the Mn-$K$ resonant scattering reflects the *tensor* susceptibility of $\mathrm{Mn}^{3+}$, the intensity should change with the polarization of the incident beam. With the alternating ordering of $\mathrm{Mn}^{3+}$ orbital configuration, the atomic scattering factor tensors are given by

$$f_1=\begin{pmatrix}\frac{f_\alpha+f_\beta}{2} & \frac{f_\alpha-f_\beta}{2} & 0\\ \frac{f_\alpha-f_\beta}{2} & \frac{f_\alpha+f_\beta}{2} & 0\\ 0 & 0 & f_\gamma\end{pmatrix},$$

$$f_2=\begin{pmatrix}\frac{f_\alpha+f_\beta}{2} & \frac{f_\beta-f_\alpha}{2} & 0\\ \frac{f_\beta-f_\alpha}{2} & \frac{f_\alpha+f_\beta}{2} & 0\\ 0 & 0 & f_\gamma\end{pmatrix}, \quad (2)$$

respectively, for the coordinate in the crystallographic axes $(\hat{a},\hat{b},\hat{c})$ in the $Pbnm$ setting. Here $f_\alpha$, $f_\beta$, and $f_\gamma$ are the three eigenvalues of the atomic susceptibility tensor of $\mathrm{Mn}^{3+}$ in a distorted $\mathrm{MnO}_6$ octahedron. With the $\sigma$-polarized incident beam, dependence of the intensity of (0,odd/2,0) orbital reflection on the azimuthal angle $\phi$, which denotes rotation around the scattering vector [see Fig. 1(b)], is represented as

$$\begin{aligned}I^{\sigma\pi'}_{0(\mathrm{odd}/2)0}&\propto|(-\sin\theta,\cos\theta,0)U(\phi)(f_1-f_2)U^{-1}(\phi)^t(0,0,1)|^2\\ &=|f_\alpha-f_\beta|^2\sin^2\phi\cos^2\theta. \end{aligned}\quad (3)$$

Here $\theta$ is the scattering angle, and the matrix

$$U(\phi)=\begin{pmatrix}\cos\phi & 0 & -\sin\phi\\ 0 & 1 & 0\\ \sin\phi & 0 & \cos\phi\end{pmatrix} \quad (4)$$

describes the azimuthal rotation of the sample around the $b$ axis. In Eq. (3) the intensity is calculated for the $\pi'$-polarized scattering beam. For the $\sigma'$ polarization one obtains $I^{\sigma\sigma'}_{0(\mathrm{odd}/2)0}=0$, replacing $(-\sin\theta,\cos\theta,0)$ with (0,0,1) in Eq. (3). The $\phi$ dependence of the (0,5/2,0) intensity at 6 K shown in Fig. 4 corresponds significantly with the calculation above. Such $\phi$ dependence has been reported for orbital-order superlattice reflections in relevant compounds $\mathrm{La}_{1/2}\mathrm{Sr}_{3/2}\mathrm{MnO}_4$ and $\mathrm{LaMnO}_3$.[7,10]

As for charge-ordering $(0,k,0)$ scattering,[11]

$$\begin{aligned}I^{\sigma\sigma'}_{0k0}&\propto|(0,0,1)U(\phi)(f_1+f_2-2f_{\mathrm{Mn}^{4+}}+C)U^{-1}(\phi)^t(0,0,1)|^2\\ &=|(f_\alpha+f_\beta-2f_{\mathrm{Mn}^{4+}}+C)\sin^2\phi\\ &\quad+(2f_\gamma-2f_{\mathrm{Mn}^{4+}}+C)\cos^2\phi|^2. \end{aligned}\quad (5)$$

Here $C=-8f_{\mathrm{O}^{2-}}\sin(\varepsilon k\pi/2)$ describes the contribution by the breathing-type displacements of oxygen atoms. The scattering factor of $\mathrm{Mn}^{4+}$, $f_{\mathrm{Mn}^{4+}}$, is assumed to be a scalar because the $3d^3_\varepsilon$ configuration holds a cubic symmetry. Note that when $\phi=\pi/2$, Eq. (5) coincides with Eq. (1) if we set $(f_\alpha+f_\beta)/2=f_{\mathrm{Mn}^{3+}}(\omega)$. Figure 4 shows the intensity of the (0,3,0) reflection for a resonant (6.555 keV) and off-resonant (6.520 keV) photon energy as a function of $\phi$. For the resonant case one can observe characteristic $\phi$ dependence. The (0,3,0) superlattice reflection in the $E\|a$ configuration is much stronger than in the $E\|c$ configuration. It is evident

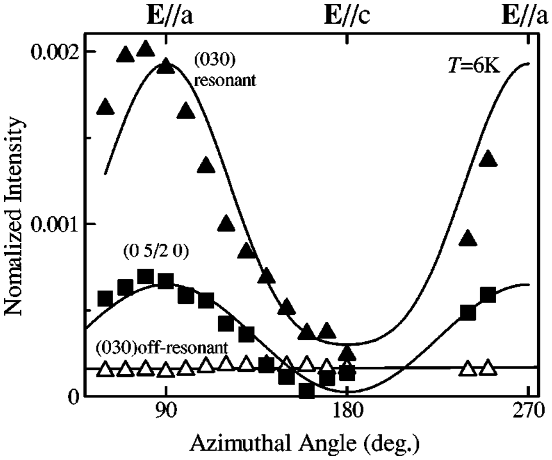

FIG. 4. Azimuthal angle dependence of the intensity of the (0,5/2,0) and (0,3,0) superlattice scattering at 6 K for a resonant photon energy (6.555 keV). The dependence of the intensity of the (0,3,0) reflection for a off-resonant photon energy (6.520 keV) is also shown with open triangles. Solid lines are the best-fitted curves using Eqs. (3) and (5).

that the value of $|f_\alpha + f_\beta - 2f_{\mathrm{Mn}^{4+}}|$ would be much larger than $|2f_\gamma - 2f_{\mathrm{Mn}^{4+}}|$, because the contribution of $C$ is relatively small for the photon energy [see Fig. 3(c)]. On the contrary, the intensity does not change beyond experimental error for the off-resonant case. It proves that an atomic scattering factor can be considered a scalar for off-resonant photon energies.

It has been reported that the $c$ axis of $\mathrm{Nd}_{1/2}\mathrm{Sr}_{1/2}\mathrm{MnO}_3$ abruptly shrinks for the charge-ordering phase,[4] while the $a$ and $b$ axes are elongated. This strongly suggests from the viewpoint of cooperative Jahn-Teller distortion that the probable orbital ordering is of $(d_{3x^2-r^2}/d_{3y^2-r^2})$ type. Thus, one can replace $f_\alpha$, $f_\beta$, and $f_\gamma$ with $f_\parallel$, $f_\perp$, and $f_\perp$, respectively. Here $f_\parallel$ $(f_\perp)$ denotes the susceptibility tensor element for the direction to which the (un)occupied $3d_\gamma$ orbital extends. To explain the $\phi$ dependence of the charge-order reflection, the relation

$$|f_\parallel - f_{\mathrm{Mn}^{4+}}| > |f_\perp - f_{\mathrm{Mn}^{4+}}| \tag{6}$$

should hold. Ishihara and Maekawa pointed out that an energy split in threefold $\mathrm{Mn}^{3+}$ $4p$ levels make the anomalous scattering factor of $\mathrm{Mn}^{3+}$ behave as a tensor.[9,11] The absorption edge of $\mathrm{Mn}^{3+}$ is a few eV lower than $\mathrm{Mn}^{4+}$. Thus, Eq. (6) indicates that the Mn $1s$–$4p_x$ excitation energy with the orbital configuration of $3d_\varepsilon^3 3d_{3x^2-r^2}$ is lower than Mn $1s$–$4p_{y,z}$. The characteristic azimuthal angle dependence of charge-ordering reflections for a resonant photon energy should be reversed in the case of the $(d_{x^2-z^2}/d_{y^2-z^2})$-type orbital ordering: the (0,3,0) reflection would be stronger in the $E\|c$ configuration than in the $E\|a$ configuration. The present work should be an important reference for determining orbital states in other related materials with the ATS technique. A possible origin of the energy split is the crystal-field splitting of Mn $4p$ levels in an $\mathrm{Mn}^{3+}\mathrm{O}_6$ octahedron with the Jahn-Teller distortion.

In conclusion, we have presented direct evidence for charge and orbital ordering in $\mathrm{Nd}_{1/2}\mathrm{Sr}_{1/2}\mathrm{MnO}_3$ by using the technique of resonant x-ray scattering. Temperature dependence was found to agree with a strong first-order phase transition. Characteristic dependence on the polarization of the incident x-ray beam was observed not only for an orbital superlattice reflection but also for a charge reflection. The dependence is ascribed to the $(d_{3x^2-r^2}/d_{3y^2-r^2})$-type orbital ordering.

The authors would like to thank S. Ishihara who first pointed out the importance of azimuthal-angle dependence of charge superlattice reflections. Also acknowledged are fruitful discussions with K. Hirota and Y. Tokura. The Cu (220) analyzer crystal was lent by D. Gibbs and J. Hill. This work was supported by the Ministry of Education, Science and Culture of Japan.

---

[1] R. M. Kusters, J. Singleton, D. A. Keen, R. McGreevy, and W. Hayes, Physica B **155**, 362 (1989); R. von Helmolt, J. Wecker, B. Holzapfel, L. Schultz, and K. Samwer, Phys. Rev. Lett. **71**, 2331 (1993); Y. Tokura, A. Urushibara, Y. Moritomo, T. Arima, A. Asamitsu, G. Kido, and N. Furukawa, J. Phys. Soc. Jpn. **63**, 3931 (1994); A. Urushibara, Y. Moritomo, T. Arima, A. Asamitsu, G. Kido, and Y. Tokura, Phys. Rev. B **51**, 14 103 (1995).

[2] E. O. Wallan and W. C. Koehlar, Phys. Rev. **100**, 545 (1955); J. B. Goodenough, *ibid.* **100**, 564 (1955).

[3] P. G. Radaelli, D. E. Cox, M. Marezio, and S-W. Cheong, Phys. Rev. B **55**, 3015 (1997).

[4] V. A. Bokov, N. A. Grigoryan, M. F. Bryzhina, and V. V. Tikhonov, Phys. Status Solidi **28**, 835 (1968).

[5] H. Kuwahara, Y. Tomioka, Y. Moritomo, A. Asamitsu, M. Kasai, and Y. Tokura, Science **270**, 961 (1995).

[6] H. Kawano, R. Kajimoto, H. Yoshizawa, Y. Tomioka, H. Kuwahara, and Y. Tokura, Phys. Rev. Lett. **78**, 4253 (1997).

[7] Y. Murakami, H. Kawada, H. Kawata, M. Tanaka, T. Arima, Y. Moritomo, and Y. Tokura, Phys. Rev. Lett. **80**, 1932 (1998).

[8] The imperfect $\pi'$ polarization of the orbital superlattice reflection can be ascribed to rotation of $\mathrm{MnO}_6$ octahedra around the $c$ axis. The intensity ratio of the two polarizations for an orbital-order reflection is given as a function of the rotating angle $\alpha$, by $I^{\sigma\sigma'}/I^{\sigma\pi'} = (\sin 2\alpha/\cos 2\alpha \cos\theta)^2$. The rotation of 15° can reproduce the data, which is comparable to the value of 9° obtained from a neutron study (Ref. 5).

[9] S. Ishihara and S. Maekawa, Phys. Rev. Lett. **80**, 3799 (1998).

[10] Y. Murakami, J. P. Hill, D. Gibbs, M. Blume, I. Koyama, M. Tanaka, H. Kawata, T. Arima, Y. Tokura, K. Hirota, and Y. Endoh, Phys. Rev. Lett. **81**, 582 (1998).

[11] S. Ishihara and S. Maekawa, Phys. Rev. B **58**, 13 442 (1998).